

PeRFlow: Piecewise Rectified Flow as Universal Plug-and-Play Accelerator

Hanshu Yan*, Xingchao Liu+, Jiachun Pan#, Jun Hao Liew*, Qiang Liu+, Jiashi Feng*

*ByteDance, +Univeristy of Texas at Austin, #National University of Singapore
hanshu.yan@bytedance.com

ABSTRACT

We present Piecewise Rectified Flow (PeRFlow), a flow-based method for accelerating diffusion models. PeRFlow divides the sampling process of generative flows into several time windows and straightens the trajectories in each interval via the reflow operation, thereby approaching piecewise linear flows. PeRFlow achieves superior performance in a few-step generation. Moreover, through dedicated parameterizations, the obtained PeRFlow models show advantageous transfer ability, serving as universal plug-and-play accelerators that are compatible with various workflows based on the pre-trained diffusion models. The implementations of training and inference are fully open-sourced.¹

1 INTRODUCTION

Diffusion models have exhibited impressive generation performances across different modalities, such as image [Rombach et al., 2022; Ho et al., 2022a; Song et al., 2021; Balaji et al., 2022], video [Ho et al., 2022b; Zhou et al., 2023; Wang et al., 2024a; Liew et al., 2023; Xu et al., 2023b], and audio [Kong et al., 2020]. Diffusion models generate samples by reversing pre-defined complicated diffusion processes, thus requiring many inference steps to synthesize high-quality results. Such expensive computational cost hinders their deployment [Li et al., 2024; Song et al., 2023; Pan et al., 2023] in real-world applications.

Diffusion models can be efficiently sampled by solving the corresponding probability flow ordinary differential equations (PF-ODEs) [Song et al., 2021; 2022]. Researchers have designed many advanced samplers, such as DDIM [Song et al., 2022], DPM-solver [Lu et al., 2022b], and DEIS [Zhang and Chen, 2022], to accelerate generation, inspired by the semi-linear structure and adaptive solvers in ODEs. However, these samplers still require tens of inference steps to generate satisfying results. Researchers have also explored distilling pretrained diffusion models into few-step generative models [Salimans and Ho, 2022; Meng et al., 2023; Gu et al., 2023; Yin et al., 2023; Nguyen and Tran, 2024], which have succeeded in synthesizing images within 8 inference steps. Progressive Distillation [Salimans and Ho, 2022] separates the whole sampling process into multiple segments and learns the mapping from starting points to endpoints for each segment. Distribution Matching Distillation [Yin et al., 2023] and SwiftBrush [Nguyen and Tran, 2024] use the score distillation loss to align the distributions of teacher and one-step student generators. UFOGen [Xu et al., 2023a], SDXL-Turbo [Sauer et al., 2023] and SDXL-Lightning [Lin et al., 2024] resort to adversarial training for learning few-step/one-step image generators. They initialize the students from pretrained diffusion models and use adversarial and/or MSE losses to align the student model’s generation with the pretrained ones. These methods suffer from the difficult tuning of the adversarial training procedure and the mode collapse issue. Latent Consistency Model (LCM) [Luo et al., 2023a;b] adopts consistency distillation [Song et al., 2023] to train a generator that directly maps noises to the terminal images. LCM only utilizes supervised distillation where the training procedure will be more stable and easier in comparison to adversarial training. However, the generated images have fewer details compared with SDXL-Lighting.

Unlike the existing methods above, which mainly learn the mappings from noises to images, we aim to simplify the flow trajectories and preserve the continuous flow trajectories of the original

¹<https://github.com/magic-research/piecewise-rectified-flow>

pretrained diffusion models. Specifically, we attempt to straighten the trajectories of the original PF-ODEs via a piecewise reflow operation. Previously, InstaFlow [Liu et al., 2023] leverages the rectified flow framework [Liu et al., 2022; Liu, 2022] to learn the transformation from initial random noise to images. It bridges the two distributions with linear interpolation and trains the model by matching the interpolation. With the reflow operation, it may be able to learn straight-line flows for one-step generation via pure supervised learning. InstaFlow provides a simple pipeline for accelerating pretrained diffusion models, however, it suffers from poor sampling quality which can be attributed to synthetic data generation. The reflow operation requires generating data from the pretrained diffusion models with ODE solvers (e.g., DDIM or DPM-Solver [Lu et al., 2022b; 2023]) to construct a training dataset. Synthesizing training data brings two problems: (1) constructing and storing the dataset requires excessive time and space, which limits its training efficiency; (2) synthetic data has a noticeable gap with real training data in quality due to the numerical error of solving ODEs. Thus, the performance of the learned straighter flow is bounded. To address the problems, *we propose piecewise rectified flow (PeRFlow), which divides the flow trajectories into several time windows and conducts reflow in each window.* By solving the ODEs in the shortened time interval, PeRFlow avoids simulating the entire ODE trajectory for preparing the training data. This significantly reduces the target synthesis time, enabling the simulation to be performed in real time along with the training procedure. Besides, PeRFlow samples the starting noises by adding random noises to clean images according to the marginal distributions, and solves the endpoints of a shorter time interval, which has a lower numerical error than integrating the entire trajectories. Through such a divide-and-conquer strategy, PeRFlow can straighten the sampling trajectories with large-scale real training data. Besides the training framework, *we also design a dedicated parameterization method for PeRFlow to inherit sufficient knowledge from the pretrained diffusion models.* Diffusion models are usually trained with ϵ -prediction, but flow-based generative models generate data by following the velocity field. We derive the correspondence between ϵ -prediction and the velocity field of flow, thus narrowing the gap between the pretrained diffusion models and the student PeRFlow model. Consequently, PeRFlow acceleration converges fast and the resultant model can synthesize highly-detailed images within very few steps. PeRFlow does not require unstable adversarial training or a complete modification of the training paradigm. It is a lightweight acceleration framework and can be easily applied to training unconditional/conditional generative models of different data modalities.

We conducted extensive experiments to verify the effectiveness of PeRFlow on accelerating pretrained diffusion models, including Stable Diffusion (SD) 1.5, SD 2.1, SDXL [Podell et al., 2023], and AnimateDiff [Guo et al., 2023]. PeRFlow-accelerated models can generate high-quality results within four steps. Moreover, we find that the variation of the weights, $\Delta W = \theta - \phi$, between the trained student model θ and the pretrained diffusion model ϕ , can serve as universal accelerators of almost all workflows that are only trained on the pretrained diffusion models. These workflows include customized SD models, ControlNets, and multiview 3D generation. We compared PeRFlow with state-of-the-art acceleration methods. PeRFlow shows advantages in terms of FID values, visual quality, and generation diversity.

In summary, PeRFlow has the following favorable features: 1) it is simple and flexible for accelerating various diffusion pipelines with fast convergence; 2) The accelerated generators support fast generation; 3) The obtained ΔW shows superior plug-and-play compatibility with the workflows of the pretrained models.

2 METHODOLOGY

2.1 RECTIFIED FLOW AND REFLOW

Flow-based generative models aim to learn a velocity field $\mathbf{v}_\theta(\mathbf{z}_t, t)$ that transports random noise $\mathbf{z}_1 \sim \pi_1$ sampled from a noise distribution into certain data distribution $\mathbf{z}_0 \sim \pi_0$. Then, one can generate samples by solving (1) from $t = 1$ to 0:

$$d\mathbf{z}_t = \mathbf{v}_\theta(\mathbf{z}_t, t)dt, \quad \mathbf{z}_1 \sim \pi_1. \quad (1)$$

Recently, simulation-free learning of flow-based models has become prevalent [Liu et al., 2022; Liu, 2022; Lipman et al., 2022; Albergo et al., 2023]. A representative method is Rectified flow [Liu et al., 2022; Liu, 2022; Lipman et al., 2022], which adopts linear interpolation between the noise distribution \mathbf{z}_1 and the data distribution \mathbf{z}_0 . It trains a neural network \mathbf{v}_θ to approximate the velocity

field via the conditional flow matching loss. The corresponding optimization procedure is termed reflow [Liu et al., 2022; Liu, 2022],

$$\min_{\theta} \mathbb{E}_{\mathbf{z}_1 \sim \pi_1, \mathbf{z}_0 \sim \pi_0} \left[\int_0^1 \|(\mathbf{z}_1 - \mathbf{z}_0) - v_{\theta}(\mathbf{z}_t, t)\|^2 dt \right], \quad \text{with } \mathbf{z}_t = (1-t)\mathbf{z}_0 + t\mathbf{z}_1. \quad (2)$$

A favorable property of the reflow operation is that, by using the optimal v_{θ^*} learned in (2) as teacher, one can repeat the reflow operation to learn a new flow-based generative model which is straighter and faster in simulation,

$$\min_{\theta'} \mathbb{E}_{\mathbf{z}_1 \sim \pi_1} \left[\int_0^1 \|(\mathbf{z}_1 - \mathbf{z}_0) - v_{\theta'}(\mathbf{z}_t, t)\|^2 dt \right], \quad (3)$$

with $\mathbf{z}_0 = \mathbf{z}_1 + \int_1^0 v_{\theta^*}(\mathbf{z}_t, t) dt$ and $\mathbf{z}_t = (1-t)\mathbf{z}_0 + t\mathbf{z}_1$.

Pretrained diffusion models can be transformed to probability flow ODEs, hence they can serve as v_{θ^*} for learning the straighter flow in (3). InstaFlow [Liu et al., 2023] proposed to accelerate pretrained diffusion-based text-to-image models via reflow. Given a pretrained diffusion model f_{ϕ} , one can generate new data by solving the corresponding probability flow ODE. We denote $\Phi(\mathbf{z}_t, t, s)$ as the ODE solver, such as the DPM-Solver [Lu et al., 2022a]. For simplicity, our notation drops the parameters in the ODE solvers. By simulating with $\Phi(\mathbf{z}_1, 1, 0)$, where \mathbf{z}_1 is sampled from the random Gaussian distribution π_1 , it synthesizes a dataset of (text, noise, image) triplets for reflow. Since it usually takes tens of inference steps to generate high-quality data with $\Phi(\mathbf{z}_1, 1, 0)$, InstaFlow is expensive to scale up. Moreover, since InstaFlow is trained with generated images, it lacks the supervision of real data and thus compromises the resulting generation quality. In the following subsections, we target solving these problems.

2.2 PIECEWISE RECTIFIED FLOW

We present Piecewise Rectified Flow (PeRFlow), aiming at training a piecewise linear flow to approximate the sampling process of a pretrained diffusion model. PeRFlow sticks to the idea of trajectory straightening. It further allows using high-quality real training data and one-the-fly optimization. PeRFlow is easier to scale up and succeeds in accelerating large-scale diffusion models, including the Stable Diffusion family.

A pretrained diffusion model f_{ϕ} corresponds to a probability flow ODE defined by a noise schedule $\sigma(t)$. In the Stable Diffusion family, the forward diffusion process follows $\mathbf{z}_t = \sqrt{1 - \sigma^2(t)}\mathbf{z}_0 + \sigma(t)\epsilon$, where \mathbf{z}_0 and ϵ are sampled from the data distribution and random Gaussian respectively. The sampling trajectories are usually complicated curves. Even for an advanced ODE solver $\Phi(\mathbf{z}_t, t, s)$, it still requires many steps to generate an artifact-free image. We accelerate the pretrained model by applying a divide-and-conquer strategy, that is, we divide the ODE trajectories into multiple time windows and straighten the trajectories in each time window via the reflow operation.

We create K time windows $\{[t_k, t_{k-1})\}_{k=K}^1$ where $1 = t_K > \dots > t_k > t_{k-1} > \dots > t_0 = 0$. For each time window $[t_k, t_{k-1})$, the starting distribution π_k will be the marginal distribution of the diffusion process at time t_k . It can be derived from $\mathbf{z}_{t_k} = \sqrt{1 - \sigma^2(t_k)}\mathbf{z}_0 + \sigma(t_k)\epsilon$. The target end distribution π_{k-1} is constructed by $\Phi(\mathbf{z}_{t_k}, t_k, t_{k-1})$. We train the PeRFlow model, denoted by θ , to fit the linear interpolation between \mathbf{z}_{t_k} and $\mathbf{z}_{t_{k-1}}$ for all $k \in [1, \dots, K]$.

$$\min_{\theta} \sum_{k=1}^K \mathbb{E}_{\mathbf{z}_{t_k} \sim \pi_k} \left[\int_{t_{k-1}}^{t_k} \left\| \frac{\mathbf{z}_{t_{k-1}} - \mathbf{z}_{t_k}}{t_{k-1} - t_k} - v_{\theta}(\mathbf{z}_t, t) \right\|^2 dt \right], \quad (4)$$

with $\mathbf{z}_{t_{k-1}} = \Phi(\mathbf{z}_{t_k}, t_k, t_{k-1})$ and $\mathbf{z}_t = \frac{t - t_{k-1}}{t_k - t_{k-1}}\mathbf{z}_{t_k} + \frac{t_k - t}{t_k - t_{k-1}}\mathbf{z}_{t_{k-1}}$.

Parameterization The pretrained diffusion models are usually trained by two parameterization tricks, namely ϵ -prediction and velocity-prediction. To inherit knowledge from the pretrained network, we parameterize the PeRFlow model as the same type of diffusion and initialize network θ from the pretrained diffusion model ϕ . For the velocity-prediction, we can train the PeRFlow model by

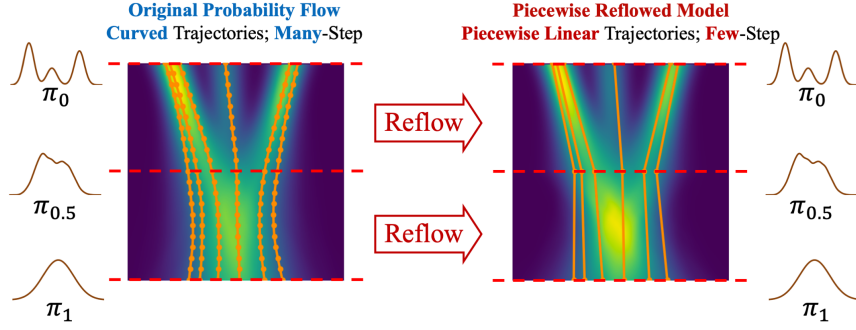


Figure 1: Our few-step generator PeRFlow is trained by a divide-and-conquer strategy. We divide the ODE trajectories into several intervals and perform reflow in each time window to straighten the sampling trajectories.

velocity-matching in (4). To accommodate ϵ -prediction, we can represent the denoised state $z_{t_{k-1}}$ with the starting state z_{t_k} and ϵ :

$$z_{t_{k-1}} = \lambda_k z_{t_k} + \eta_k \epsilon, \quad (5)$$

where $\lambda_k > 1$ and η_k are defined by the user. We propose to train a neural network $\epsilon_\theta(z_t, t)$ to estimate the noise ϵ in (5) based on z_t for all $t \in [t_k, t_{k-1}]$:

$$\min_{\theta} \sum_{k=1}^K \mathbb{E}_{z_{t_k} \sim \pi_k} \left[\int_{t_{k-1}}^{t_k} \left\| \frac{z_{t_{k-1}} - \lambda_k z_{t_k}}{\eta_k} - \epsilon_\theta(z_t, t) \right\|^2 dt \right], \quad (6)$$

$$\text{with } z_{t_{k-1}} = \Phi(z_{t_k}, t_k, t_{k-1}) \quad \text{and} \quad z_t = \frac{t - t_{k-1}}{t_k - t_{k-1}} z_{t_k} + \frac{t_k - t}{t_k - t_{k-1}} z_{t_{k-1}}.$$

The optimum of (4) and (6) are,

$$v^*(z_t, t) = \mathbb{E} \left[\frac{z_{t_{k-1}} - z_{t_k}}{t_{k-1} - t_k} \middle| z_t \right], \quad \text{and} \quad \epsilon^*(z_t, t) = \mathbb{E} \left[\frac{z_{t_{k-1}} - \lambda_k z_{t_k}}{\eta_k} \middle| z_t \right].$$

Using calculus and the fact $z_t = \frac{t - t_{k-1}}{t_k - t_{k-1}} z_{t_k} + \frac{t_k - t}{t_k - t_{k-1}} z_{t_{k-1}}$, we get,

$$v^*(z_t, t) = \frac{(1 - \lambda_k) z_t - \eta_k \epsilon^*(z_t, t)}{t - t_{k-1} + \lambda_k t_k - \lambda_k t} \quad (7)$$

The sampling process involves first computing $\epsilon_\theta(z_t, t)$ from z_t , then estimating the velocity $v(z_t)$ via (7) for solving the ODE (1). In this paper, we consider two choices for λ and η :

- *Parameterization [A]*: Since $z_{t_k} = \sqrt{1 - \sigma_k^2} z_0 + \sigma_k \epsilon$ and $z_{t_{k-1}} = \sqrt{1 - \sigma_{k-1}^2} z_0 + \sigma_{k-1} \epsilon$, given the same random noise ϵ and data z_0 , we can represent z_{t_k} with $z_{t_{k-1}}$ and yield,

$$\lambda_k = \frac{\sqrt{1 - \sigma_{k-1}^2}}{\sqrt{1 - \sigma_k^2}}, \quad \eta_k = -\frac{\sqrt{\sigma_k^2 - \sigma_{k-1}^2}}{\sqrt{1 - \sigma_k^2}}. \quad (8)$$

- *Parameterization [B]*: We can also follow the DDIM solver [Song et al., 2022], i.e.,

$$z_{t_{k-1}} = \sqrt{\frac{\alpha_{t_{k-1}}}{\alpha_{t_k}}} z_{t_k} + \sqrt{\alpha_{t_{k-1}}} \left(\sqrt{\frac{1 - \alpha_{t_{k-1}}}{\alpha_{t_{k-1}}}} - \sqrt{\frac{1 - \alpha_{t_k}}{\alpha_{t_k}}} \right) \epsilon_\theta(z_{t_k}, t_k),$$

where $\alpha_k = 1 - \sigma_k^2$. We can correspondingly set,

$$\lambda_k = \frac{\sqrt{\alpha_{k-1}}}{\sqrt{\alpha_k}}, \quad \eta_k = \sqrt{1 - \alpha_{k-1}} - \frac{\sqrt{\alpha_{k-1}}}{\sqrt{\alpha_k}} \sqrt{1 - \alpha_k}. \quad (9)$$

This parameterization initializes the student flow from the update rule of DDIM, which is equivalent to the Euler discretization of the probability flow ODE. We empirically observe that it gives faster training convergence.

Scaling Up with Real Training Data PeRFlow divides the time range $[1, 0]$ into multiple windows. For each window, the starting point z_{t_k} is obtained by adding random noise to *real* training data z_0 , and it only requires several inference steps to solve the ending point $z_{t_{k-1}}$. The computational cost is significantly reduced for each training iteration compared to InstaFlow, allowing us to train PeRFlow on large-scale training datasets with fast online simulation of the ODE trajectory. Besides, solving endpoints of a shorter time window $[z_{t_k}, z_{t_{k-1}})$ has lower numerical errors in comparison to the entire time range. High-quality supervision yields significant improvement in the generation results.

Classifier-Free Guidance in Training Classifier-free guidance (CFG) [Ho and Salimans, 2021] is a common technique to improve the generation quality of text-to-image models. During training, we solve the endpoints $z_{t_{k-1}}$ for each time window $[t_k, t_{k-1})$ in an online manner via an ODE solver $\Phi(z_{t_k}, t_k, t_{k-1}, c, w)$, where $w \geq 1$ denotes the CFG scale, c denotes the text prompt. CFG is turned off when $w = 1$. PeRFlow supports two modes: *CFG-sync* and *CFG-fixed*:

- *CFG-sync*: We disable CFG by setting $w = 1$ for $\Phi(z_{t_k}, t_k, t_{k-1}, c, w)$. The obtained PeRFlow model can use similar CFG scales as the pretrained diffusion models to guide the sampling.
- *CFG-fixed*: We use a pre-defined $w = w^* > 1$ for $\Phi(z_{t_k}, t_k, t_{k-1}, c, w)$ during training. The obtained PeRFlow model learns to straighten the specific ODE trajectories corresponding to $\Phi(z_{t_k}, t_k, t_{k-1}, c, w^*)$. One should use a smaller CFG scale (e.g., 1.0-2.5) to adjust guidance when sampling from PeRFlow trained with *CFG-fixed*.

Through empirical comparison, we observe that PeRFlow+*CFG-sync* preserves the sampling diversity of the original diffusion models with occasional failure in generating complex structures, while PeRFlow+*CFG-fixed* trades off sampling diversity in exchange for fewer failure cases.

Our recommendations are as follows: When using powerful pre-trained diffusion models (e.g., SDXL) and prioritizing generation quality, PeRFlow+*CFG-fixed* is the better choice. On the other hand, when the goal is to maintain the sampling diversity and adaptability of customized fine-tuned plug-ins, such as Dreamshaper, PeRFlow+*CFG-sync* is the more suitable option.

PeRFlow as Universal Plug-and-Play Accelerator PeRFlow initializes the weights of the student model θ with the pretrained diffusion model ϕ . After training with piecewise reflow, we find that the change of weights $\Delta W = \theta - \phi$ can be used to seamlessly accelerate many other workflows pretrained with the diffusion model. For example, ΔW of PeRFlow+SD-v1.5 can accelerate the ControlNets [Zhang and Agrawala, 2023], IP-Adaptor [Ye et al., 2023] and multiview generation [Long et al., 2023] pipelines trained with the original SD v1.5. The accelerated pipelines achieve nearly lossless few-step generation as the original many-step generation. Please refer to Section 3.3 for detailed results.

3 EXPERIMENTS

We use PeRFlow to accelerate several large-scale text-to-image and text-to-video models, including SD-v1.5, SD-v2.1, SDXL, and AnimateDiff. In this section, we will illustrate the experiment configurations and empirical results.

Experiment Configuration All the PeRFlow models are initialized from their diffusion teachers. PeRFlow-SD-v1.5 is trained with images in resolution of 512×512 using ϵ -prediction defined in (8). PeRFlow-SD-v2.1 is trained with images in resolution of 768×768 using v -prediction. PeRFlow-SDXL is trained with images in resolution of 1024×1024 using ϵ -prediction defined in (9). Images are all sampled from the LAION-Aesthetics-5+ dataset [Schuhmann et al., 2022] and center-cropped. We also train PeRFlow-AnimateDiff with video clips in size of $16 \times 384 \times 384$ using ϵ -prediction defined in (9). We randomly drop out the text captions with a low probability (10%) to enable classifier-free guidance during sampling. We divide the time range $[0, 1]$ into four windows uniformly. For each window, we use the DDIM solver to solve the endpoints with 8 steps. We refer to the Hugging Face scripts for training Stable Diffusion ² to set other hyper-parameters, including learning rate and weight decay.

²https://github.com/huggingface/diffusers/tree/main/examples/text_to_image

Algorithm 1: Piecewise Rectified Flow

```

1 Input: Training dataset  $\mathcal{D}$ ,  $\epsilon$ - or  $\nu$ -prediction teacher model  $f_\phi$ , Noise schedule  $\sigma(t)$ , ODE
  solver  $\Phi(z_t, t, s, f_\phi)$ , Number of windows  $K$ , student model  $\epsilon_\theta$  or  $\nu_\theta$ ,
2 Create  $K$  time windows  $\{(t_{k-1}, t_k)\}_{k=1}^K$  with  $t_K = 1$  and  $t_0 = 0$ ;
3 Initialize  $\theta = \phi$ ;
4 repeat
5   Sample  $z_0 \sim \mathcal{D}$ ;
6   Sample  $k$  from  $\{1, \dots, K\}$  uniformly, then randomly sample time  $t \in (t_{k-1}, t_k]$ ;
7   Sample random noise  $\epsilon \sim \mathcal{N}(\mathbf{0}, \mathbf{I})$ ;
8   Get  $z_{t_k} = \sqrt{1 - \sigma^2(t_k)}z_0 + \sigma(t_k)\epsilon$ ;
9   Solve the endpoint of the time window  $z_{t_{k-1}} = \Phi(z_{t_k}, t_k, t_{k-1})$ ;
10  Get  $z_t = z_{t_k} + \frac{z_{t_k} - z_{t_{k-1}}}{t_k - t_{k-1}}(t - t_k)$ ;
11  if  $\epsilon$ -prediction then
12    Compute loss  $\ell = \left\| \epsilon_\theta(z_t, t) - \frac{z_{t_{k-1}} - \lambda_k z_{t_k}}{\eta_k} \right\|^2$ ;
13  else
14    Compute loss  $\ell = \left\| \nu_\theta(z_t, t) - \frac{z_{t_k} - z_{t_{k-1}}}{t_k - t_{k-1}} \right\|^2$ ;
15  end
16  Update  $\theta$  with gradient-based optimizer using  $\nabla_\theta \ell$ .
17 until convergence;
18  $\Delta W = \theta - \phi$ .
19 Return: Fast PeRFlow  $f_\theta$  and  $\Delta W$ .

```

3.1 FEW-STEP GENERATION

PeRFlow succeeds in accelerating pretrained Stable Diffusion models to few-step generators. As shown in figure 4, 5, and 3, PeRFlow can generate astonishing pictures with only 4 steps. If increasing the number of inference steps (e.g., 6 and 8), we can obtain images with much richer details as shown in figure 7. We compare the generation results with two SOTA methods, LCM-LORA and SDXL-lightning. PeRFlow enjoys richer visual details, refer to figure 2.

We compute the FID values of PeRFlow-SD-v1.5 in table 1. We randomly sample 30k images from LAION-5B-Aesthetics as the reference set and generate the same number of images via the PeRFlow model with 4/8 steps as the test sets. We also compute the FID values by using COCO2014 as the reference distributions. In comparison to LCM-LORA, we observe that PeRFlow models have obviously lower FID values. When increasing the number of inference steps, the FID values of PeRFlow will decrease because the numerical errors of solving sampling ODE are better controlled. However, the FID values of LCM-LORA unexpectedly increase.

	LAION-5B		COCO2014		SD-v1.5	
FID	4-step	8-step	4-step	8-step	4-step	8-step
PeRFlow	9.74	8.62	11.31	14.16	9.46	5.05
LCM-LORA	15.28	19.21	23.49	29.63	15.63	21.19

Table 1: FID values of PeRFlow-SD-v1.5

3.2 DOMAIN SHIFT CAUSED BY ACCELERATION

Diffusion acceleration aims to speed up the sampling process of the pretrained models and simultaneously preserves their performance and properties. We compute the FID values between the generation of the original SD-v1.5 and the acceleration methods. From table 1, we observe the FID values of PeRFlow are smaller than LCM-LORA. If using more inference steps, the FID values of PeRFlow



(a) LCM-LORA for SDXL

(b) SDXL-lightning

(c) PeRFlow for SDXL

Figure 2: Images (1024×1024) generated by PeRFlow enjoy richer details and texture in comparison to other acceleration methods. Prompt-1: “A closeup face photo of girl, wearing a raincoat, in the street, heavy rain, bokeh”; Prompt-2: “A closeup face photo of a boy in white shirt standing on the grassland, flowers”; Prompt-3: “A beautiful cat bask in the sun”.

will further drop. This implies the distribution shift to the original SD caused by PeRFlow is much smaller than LCM-LORA. The numerical comparison corresponds to the results in figure 8. The color style and layout of PeRFlow’s results match the results of the pretrained models, while an obvious domain shift appears in the results of LCM-LORA. Besides, the sampling diversity of PeRFlow is similar to the original SD-v1.5 and looks better than LCM-LORA in figure 9.

3.3 UNIVERSAL ACCELERATION TO SD WORKFLOWS

PeRFlow- ΔW serves as a universal accelerator that can be simply plugged into various pipelines based on the pretrained Stable Diffusion models including ControlNet [Zhang and Agrawala, 2023], IP-Adaptor [Ye et al., 2023], and multiview-generation. For example, we plug PeRFlow- ΔW into the SD-v1.5 ControlNet-Tile, this enables a 4-step image enhancement module, see figure 10. Using together with the 4-step PeRFlow T2I, we can generate high-quality 1024×1024 images with lightweight SD-v1.5 backbones. For multiview-generation, we plug PeRFlow- ΔW into the Wonder3D [Long et al., 2023] pipeline. Surprisingly, we can generate clear multiview images with only one step, see figure 11. More results are shown in figure 13, 12.



Figure 3: 4-step sampling (1024×1024) via PeRFlow-SDXL.

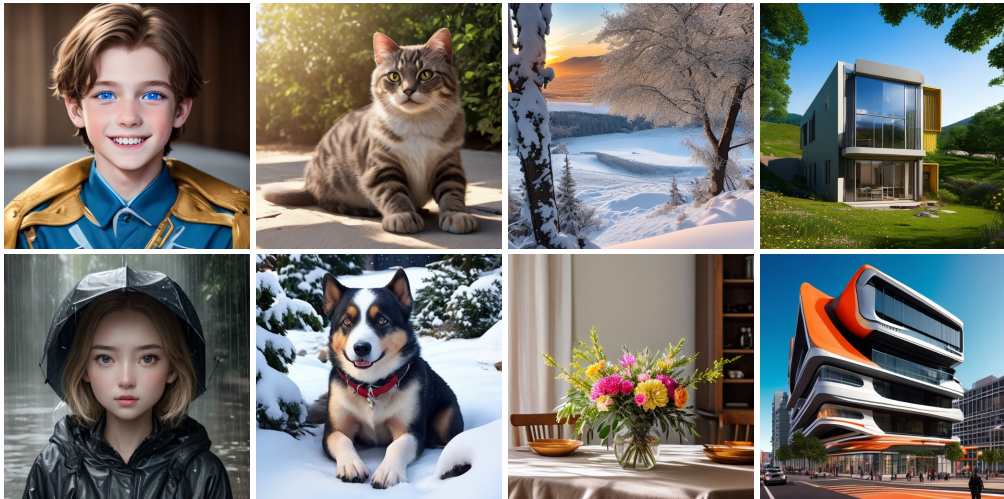


Figure 4: 4-step sampling (512×512) via PeRFlow-SD-v1.5.



Figure 5: 4-step sampling (768×768) via PeRFlow-SD-v2.1.



Figure 6: 6-step sampling ($16 \times 512 \times 512$) via PeRFlow-AnimateDiff (motion module-v3 with DreamShaper as the 2D base). The text prompts used are “A young woman smiling, in the park, sunshine” and “A dog sitting in the garden, snow, trees”. We append “4k uhd, high quality, masterpiece” as the prefix of prompts, and use “distorted, blur, haze, warm, over-saturated, worst quality, low quality, letterboxed” as the negative prompt.

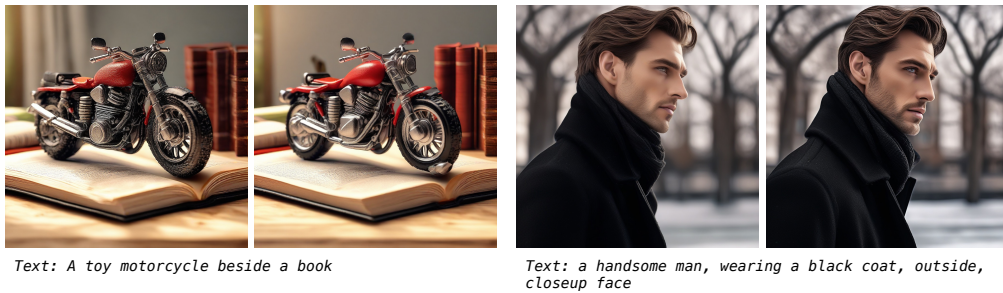


Figure 7: Comparison between 4-step (left) and 5-step (right) generation of PeRFlow-SDXL.



Figure 8: PeRFlow has better compatibility with customized SD models compared to LCM-LORA. The top is [ArchitectureExterior](#) and the bottom is [DisneyPixarCartoon](#).

3.4 INFERENCE BUDGET ALLOCATION AND DYNAMIC CFG

Suppose PeRFlow divides the entire sampling time range into K windows, K -step inference (one for each window) will yield high-quality images in most cases. For some pictures with complex structures, like motorcycles with well-crafted wheels and engines, PeRFlow may require more steps.

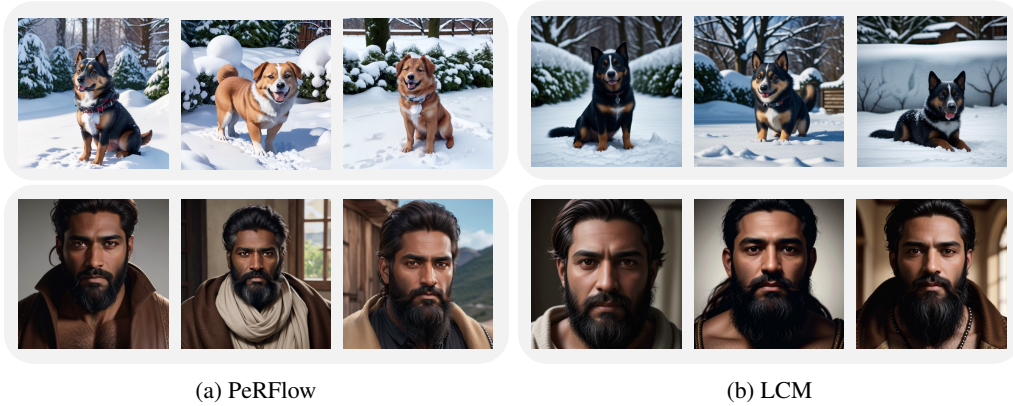


Figure 9: PeRFlow has better sampling diversity compared to LCM-LORA.



Figure 10: Fast (4-step) image refinement (128×128 to 1024×1024) via PeRFlow-ControlNet-tile.



Figure 11: PeRFlow works compatibility with Wonder3D.

Ho et al. [2020] found that diffusion models generate images by synthesizing the layout and structure first and then refining the local details. Inspired by this observation, we allocate the extra required steps to windows in highly noisy regions. Specifically, we have the K time windows $\{[t_k, t_{k-1}]\}_{k=K}^1$ with $1 = t_K > \dots > t_k > t_{k-1} > \dots > t_0 = 0$. Let the number of inference steps be $N \leq 2K$, we allocate $N//K + 1$ steps for window $[t_k, t_{k-1}]$ if $K - k < N\%K$, otherwise $N//K$. In practice, PeRFlow creates 4 time windows for acceleration training, and 5-step inference can consistently generate high-quality images.

CFG is a useful technique to improve the layout, structure, and text alignment of the generated images. However, a large CFG scale sometimes leads to over-saturated color blocks [Kynkäänniemi et al., 2024; Wang et al., 2024b]. To mitigate this issue, we use a dynamic CFG strategy for few-step sampling, i.e., the corresponding CFG scales decrease for window K to 1. For example, when sampling with 5 steps, the CFG schedule is 7.5-4.0-4.0-4.0 for the *CFG-sync* mode and 2.5-1.5-1.5-1.5 for the *CFG-fixed* mode.

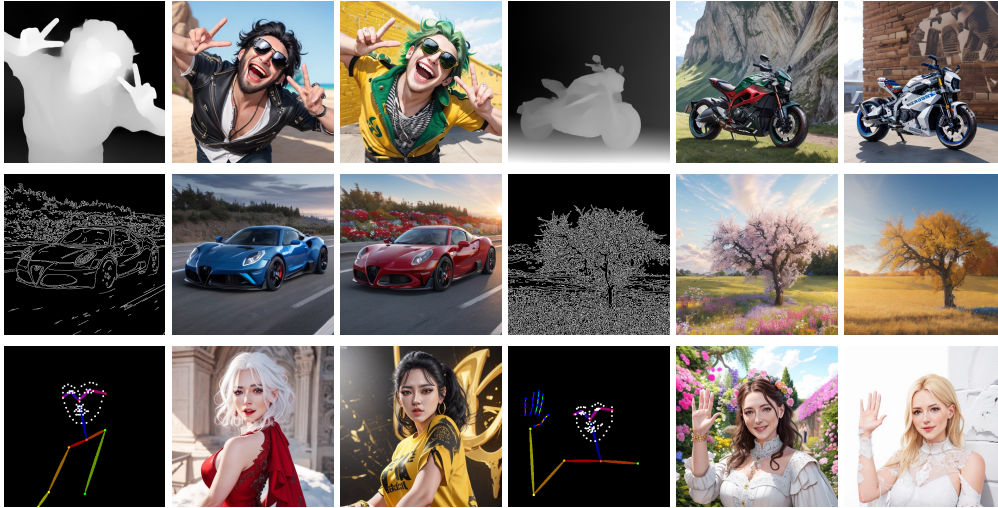


Figure 12: Fast generation via PeRFlow accelerated depth-/edge-/pose-ControlNet



Figure 13: PeRFlow works compatibility with IP-Adaptor.

REFERENCES

- M. S. Albergo, N. M. Boffi, and E. Vanden-Eijnden. Stochastic interpolants: A unifying framework for flows and diffusions. *arXiv preprint arXiv:2303.08797*, 2023.
- Y. Balaji, S. Nah, X. Huang, A. Vahdat, J. Song, Q. Zhang, K. Kreis, M. Aittala, T. Aila, S. Laine, et al. ediff-i: Text-to-image diffusion models with an ensemble of expert denoisers. *arXiv preprint arXiv:2211.01324*, 2022.
- J. Gu, S. Zhai, Y. Zhang, L. Liu, and J. M. Susskind. Boot: Data-free distillation of denoising diffusion models with bootstrapping. In *ICML 2023 Workshop on Structured Probabilistic Inference {\&} Generative Modeling*, 2023.
- Y. Guo, C. Yang, A. Rao, Y. Wang, Y. Qiao, D. Lin, and B. Dai. Animatediff: Animate your personalized text-to-image diffusion models without specific tuning. *arXiv preprint arXiv:2307.04725*, 2023.
- J. Ho and T. Salimans. Classifier-free diffusion guidance. In *NeurIPS 2021 Workshop on Deep Generative Models and Downstream Applications*, 2021.
- J. Ho, A. Jain, and P. Abbeel. Denoising Diffusion Probabilistic Models, Dec. 2020. arXiv:2006.11239 [cs, stat].
- J. Ho, C. Saharia, W. Chan, D. J. Fleet, M. Norouzi, and T. Salimans. Cascaded diffusion models for high fidelity image generation. *Journal of Machine Learning Research*, 23(47):1–33, 2022a.
- J. Ho, T. Salimans, A. Gritsenko, W. Chan, M. Norouzi, and D. J. Fleet. Video diffusion models. *Advances in Neural Information Processing Systems*, 35:8633–8646, 2022b.
- Z. Kong, W. Ping, J. Huang, K. Zhao, and B. Catanzaro. Diffwave: A versatile diffusion model for audio synthesis. *arXiv preprint arXiv:2009.09761*, 2020.

- T. Kynkäänniemi, M. Aittala, T. Karras, S. Laine, T. Aila, and J. Lehtinen. Applying guidance in a limited interval improves sample and distribution quality in diffusion models. *arXiv preprint arXiv:2404.07724*, 2024.
- Y. Li, H. Wang, Q. Jin, J. Hu, P. Chemerys, Y. Fu, Y. Wang, S. Tulyakov, and J. Ren. Snapfusion: Text-to-image diffusion model on mobile devices within two seconds. *Advances in Neural Information Processing Systems*, 36, 2024.
- J. H. Liew, H. Yan, J. Zhang, Z. Xu, and J. Feng. Magicedit: High-fidelity and temporally coherent video editing. *arXiv preprint arXiv:2308.14749*, 2023.
- S. Lin, A. Wang, and X. Yang. Sdxl-lightning: Progressive adversarial diffusion distillation, 2024.
- Y. Lipman, R. T. Chen, H. Ben-Hamu, M. Nickel, and M. Le. Flow matching for generative modeling. In *The Eleventh International Conference on Learning Representations*, 2022.
- Q. Liu. Rectified flow: A marginal preserving approach to optimal transport. *arXiv preprint arXiv:2209.14577*, 2022.
- X. Liu, C. Gong, and Q. Liu. Flow straight and fast: Learning to generate and transfer data with rectified flow. *arXiv preprint arXiv:2209.03003*, 2022.
- X. Liu, X. Zhang, J. Ma, J. Peng, et al. InstafLOW: One step is enough for high-quality diffusion-based text-to-image generation. In *The Twelfth International Conference on Learning Representations*, 2023.
- X. Long, Y.-C. Guo, C. Lin, Y. Liu, Z. Dou, L. Liu, Y. Ma, S.-H. Zhang, M. Habermann, C. Theobalt, et al. Wonder3d: Single image to 3d using cross-domain diffusion. *arXiv preprint arXiv:2310.15008*, 2023.
- C. Lu, Y. Zhou, F. Bao, J. Chen, C. Li, and J. Zhu. Dpm-solver: A fast ode solver for diffusion probabilistic model sampling in around 10 steps. *Advances in Neural Information Processing Systems*, 35:5775–5787, 2022a.
- C. Lu, Y. Zhou, F. Bao, J. Chen, C. Li, and J. Zhu. DPM-Solver: A Fast ODE Solver for Diffusion Probabilistic Model Sampling in Around 10 Steps, Aug. 2022b. *arXiv:2206.00927* [cs, stat].
- C. Lu, Y. Zhou, F. Bao, J. Chen, C. Li, and J. Zhu. Dpm-solver++: Fast solver for guided sampling of diffusion probabilistic models, 2023.
- S. Luo, Y. Tan, L. Huang, J. Li, and H. Zhao. Latent consistency models: Synthesizing high-resolution images with few-step inference, 2023a.
- S. Luo, Y. Tan, S. Patil, D. Gu, P. von Platen, A. Passos, L. Huang, J. Li, and H. Zhao. Lcm-lora: A universal stable-diffusion acceleration module, 2023b.
- C. Meng, R. Rombach, R. Gao, D. Kingma, S. Ermon, J. Ho, and T. Salimans. On distillation of guided diffusion models. In *Proceedings of the IEEE/CVF Conference on Computer Vision and Pattern Recognition*, pages 14297–14306, 2023.
- T. H. Nguyen and A. Tran. Swiftbrush: One-step text-to-image diffusion model with variational score distillation, 2024.
- J. Pan, H. Yan, J. H. Liew, V. Y. Tan, and J. Feng. Adjointdpm: Adjoint sensitivity method for gradient backpropagation of diffusion probabilistic models. *arXiv preprint arXiv:2307.10711*, 2023.
- D. Podell, Z. English, K. Lacey, A. Blattmann, T. Dockhorn, J. Müller, J. Penna, and R. Rombach. Sdxl: Improving latent diffusion models for high-resolution image synthesis. *arXiv preprint arXiv:2307.01952*, 2023.
- R. Rombach, A. Blattmann, D. Lorenz, P. Esser, and B. Ommer. High-Resolution Image Synthesis with Latent Diffusion Models, Apr. 2022. *arXiv:2112.10752* [cs].

- T. Salimans and J. Ho. PROGRESSIVE DISTILLATION FOR FAST SAMPLING OF DIFFUSION MODELS. page 21, 2022.
- A. Sauer, D. Lorenz, A. Blattmann, and R. Rombach. Adversarial diffusion distillation. *arXiv preprint arXiv:2311.17042*, 2023.
- C. Schuhmann, R. Beaumont, R. Vencu, C. Gordon, R. Wightman, M. Cherti, T. Coombes, A. Katta, C. Mullis, M. Wortsman, et al. Laion-5b: An open large-scale dataset for training next generation image-text models. *Advances in Neural Information Processing Systems*, 35:25278–25294, 2022.
- J. Song, C. Meng, and S. Ermon. Denoising Diffusion Implicit Models, June 2022. arXiv:2010.02502 [cs].
- Y. Song, J. Sohl-Dickstein, D. P. Kingma, A. Kumar, S. Ermon, and B. Poole. SCORE-BASED GENERATIVE MODELING THROUGH STOCHASTIC DIFFERENTIAL EQUATIONS. page 36, 2021.
- Y. Song, P. Dhariwal, M. Chen, and I. Sutskever. Consistency models. *arXiv preprint arXiv:2303.01469*, 2023.
- W. Wang, J. Liu, Z. Lin, J. Yan, S. Chen, C. Low, T. Hoang, J. Wu, J. H. Liew, H. Yan, et al. Magicvideo-v2: Multi-stage high-aesthetic video generation. *arXiv preprint arXiv:2401.04468*, 2024a.
- X. Wang, N. Dufour, N. Andreou, M.-P. Cani, V. F. Abrevaya, D. Picard, and V. Kalogeiton. Analysis of classifier-free guidance weight schedulers. *arXiv preprint arXiv:2404.13040*, 2024b.
- Y. Xu, Y. Zhao, Z. Xiao, and T. Hou. Ufogen: You forward once large scale text-to-image generation via diffusion gans. *arXiv preprint arXiv:2311.09257*, 2023a.
- Z. Xu, J. Zhang, J. H. Liew, H. Yan, J.-W. Liu, C. Zhang, J. Feng, and M. Z. Shou. Magicanimate: Temporally consistent human image animation using diffusion model. *arXiv preprint arXiv:2311.16498*, 2023b.
- H. Ye, J. Zhang, S. Liu, X. Han, and W. Yang. Ip-adapter: Text compatible image prompt adapter for text-to-image diffusion models. *arXiv preprint arXiv:2308.06721*, 2023.
- T. Yin, M. Gharbi, R. Zhang, E. Shechtman, F. Durand, W. T. Freeman, and T. Park. One-step diffusion with distribution matching distillation, 2023.
- L. Zhang and M. Agrawala. Adding Conditional Control to Text-to-Image Diffusion Models, Feb. 2023. arXiv:2302.05543 [cs].
- Q. Zhang and Y. Chen. Fast sampling of diffusion models with exponential integrator. *arXiv preprint arXiv:2204.13902*, 2022.
- D. Zhou, W. Wang, H. Yan, W. Lv, Y. Zhu, and J. Feng. MagicVideo: Efficient Video Generation With Latent Diffusion Models, May 2023. arXiv:2211.11018 [cs].